A Two-Dimensional Shear Spring Element

A. S. Kuo*
Fairchild Republic Company, Farmingdale, New York

A new, two-dimensional continuous shear spring element was developed to calculate the stress intensity factors in adhesively bonded structures. The quadratic quadrilateral isoparametric element was adopted to explain the formulation of element stiffness. In contrast to the conventional discrete shear spring element, the new element takes into account the continuous nature of load transfer between cracked and uncracked adherends. The capability of the new element was validated with experimental data from four types of adhesively bonded specimens. The new element is also applicable to modeling the core of honeycomb sandwich structures.

I. Introduction

ADHESIVE bonding is an attractive joining technique for the fabrication of metallic and composite airframe structures because of its manufacturing cost advantage and increased fracture resistance compared to the mechanical fastening system. In the fracture analysis of adhesively bonded structures, and adhesive layer is often modeled as discrete shear springs to simplify the calculation of stress intensity factors. The shear spring model is used in either the analytic solution or finite element analysis. Ratwani[1] recommends that the analytic solution be used for parametric studies, whereas the finite element analysis should be used for detailed analysis where more accurate stress intensity factors can be obtained.

In the finite element analysis of adhesively bonded structures, the adhesive layer is usually modeled as discrete shear spring elements that can sustain only shear forces. Figure 1 shows an example of the shear spring model for an adhesively bonded specimen that has a central crack in one of the two adherends. The adherends can be metals and/or composites. The spring constant can be calculated, as follows, with the aid of Fig. 2.

$$\tau = G\gamma \tag{1}$$

where

$$\tau = \text{shear stress} = F/A \tag{2}$$

$$\gamma = \text{shear strain} = \Delta V/h \tag{3}$$

and G is the shear modulus of adhesive, F the shear force, A the in-plane area of the element, h the adhesive thickness, and V the displacement. By substituting Eqs. (2) and (3) into Eq. (1), one obtains

$$F = (AG/h)(\Delta V) = k(\Delta V) \tag{4}$$

where

$$k = AG/h = \text{spring const} \tag{5}$$

Equation (5) shows that prescribed in-plane areas of the adhesive layer must be allocated to nodal points so that spring constants can be calculated. The allocation of in-plane area is related to the finite element mesh size, which needs to be quite small in order to obtain reasonable accuracy of the stress intensity factors. It takes a great deal of time for allocation and spring constant calculation, which are required as input data to the finite element program. Furthermore, the adhesive layer is continuous, whereas the shear spring is discrete; therefore, the load transfer between cracked and uncracked adherends may not be modeled realistically without considering the continuous nature of the adhesive layer.

In this paper, the development of a two-dimensional (2-D) continuous shear spring element is addressed. The new element does not require the preprocessing calculation of spring constants, the element realistically models the load transfer by considering the continuous nature of the adhesive layer.

II. Theoretical Formulation

The eight-node quadratic quadrilateral isoparametric element is selected to explain the formulation of element stiffness of the new 2-D shear spring element. The principles described herein can also be applied to the other types of elements.

Figure 3 shows an undeformed 2-D shear spring element that has 16 nodal points. Although the figure shows the element with a physical depth equal to the adhesive thickness, the grid points on the top surface, which is defined by grid points 9, 10, 11, and 12, have the same coordinates as the corresponding grid points on the bottom surface, which is defined by grid points 1, 2, 3, and 4. The top and bottom surfaces of the element coincide with the adherends. The depth of the element is required merely to calculate the spring constant; therefore, it is conceptually fictitious. The major difference between the discrete spring element and the new 2-D spring element is that the springs are distributed continuously between the top and bottom surfaces in the new 2-D

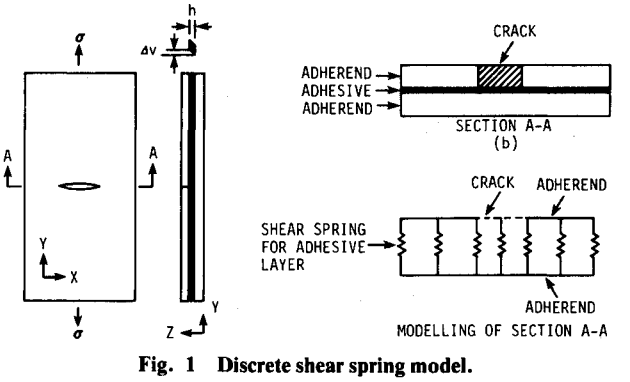

Fig. 1 Discrete shear spring model.

Submitted Jan. 31, 1983; revision submitted Nov. 3, 1983.

*Senior Engineer III.

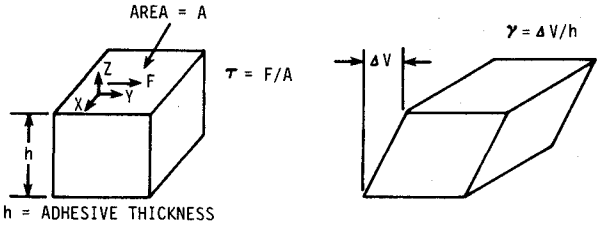

Fig. 2 Shear deformation of adhesive layer.

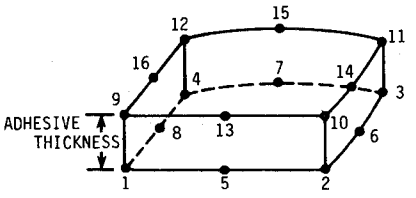

Fig. 3 New two-dimensional shear spring element.

spring element. Thus, the load transfer behavior of the adhesive layer can be more realistically modeled, and the spring constants can be calculated as an integral part of finite element program in lieu of a preprocessing effort.

The prescribed displacement distributions on the top and bottom surfaces of the 2-D spring element are given as:

$$\underset{\text{top surface}}{\begin{Bmatrix} U \\ V \end{Bmatrix}} = [N_i] \begin{Bmatrix} U_1 \\ V_1 \\ U_2 \\ V_2 \\ \vdots \\ U_7 \\ V_7 \\ U_8 \\ V_8 \end{Bmatrix} \tag{6}$$

$$\underset{\text{bottom surface}}{\begin{Bmatrix} U \\ V \end{Bmatrix}} = [N_i] \begin{Bmatrix} U_9 \\ V_9 \\ U_{10} \\ V_{10} \\ \vdots \\ U_{15} \\ V_{15} \\ U_{16} \\ V_{16} \end{Bmatrix} \tag{7}$$

where $U_1, U_2 \ldots U_{16}$ and $V_1, V_2 \ldots V_{16}$ are displacements of nodal points. The shape function N_i in Eqs. (6) and (7) for the quadratic element is available from Ref. 2. The coordinates of the points on and within element boundaries are defined as

$$X = \sum_{i=1}^{8} N_i X_i, \qquad Y = \sum_{i=1}^{8} N_i Y_i \tag{8}$$

where (X_i, Y_i) are the coordinates of the eight nodal points on each of the top and bottom surfaces shown in Fig. 3. It should be noted that this 2-D shear spring element is an isoparametric element. Thus, it can accurately model a curved structural boundary, e.g., fastener hole, with only a few elements.

The shear strain γ_{zx} and γ_{zy} of an element is

$$\{\gamma\} = \begin{Bmatrix} \gamma_{zx} \\ \gamma_{zy} \end{Bmatrix} = \frac{1}{h} \begin{Bmatrix} U_{\text{top}} - U_{\text{bottom}} \\ V_{\text{top}} - V_{\text{bottom}} \end{Bmatrix} = [B]\{\delta\} \tag{9}$$

$$\{\gamma\} = [B]\{\delta\} = \frac{1}{h}$$

$$\times \underset{[B]}{\underset{(2\times 32)}{\begin{bmatrix} N_1\ 0\ N_2\ 0 \ldots N_8\ 0 & -N_1\ 0 & -N_2\ 0 \ldots -N_8\ 0 \\ 0\ N_1\ 0\ N_2 \ldots 0\ N_8 & 0\ -N_1 & 0\ -N_2 \ldots 0\ -N_8 \end{bmatrix}}}$$

$$\times \underset{\{\delta\}}{\underset{(32\times 1)}{\begin{Bmatrix} U_1 \\ V_1 \\ U_2 \\ V_2 \\ \vdots \\ U_{15} \\ V_{15} \\ U_{16} \\ V_{16} \end{Bmatrix}}} \tag{10}$$

The equation for the element stiffness matrix can be expressed as

$$[K] = \int_{-1}^{1} [B]^T [D] [B] \det [J] \, d\xi d\eta \tag{11}$$

where $[J]$ is the Jacobian for the coordinate transformation and $[D]$ is the constitutive matrix for the adhesive layer,

$$[D] = \begin{bmatrix} G & 0 \\ 0 & G \end{bmatrix} \tag{12}$$

where G is the elastic shear modulus of the adhesive.

Equation (12) can be evaluated numerically with the nine-point Gaussian integration procedure. Since the shape function N_i is an incomplete third-degree polynomial, Eq. (10) shows that the shear strain distribution in an adhesive layer will also be an incomplete third-degree polynomial that can adequately handle high-stress gradients even with coarse mesh size.

In the formulation of element stiffness, the adhesive layer is considered as an elastic medium. Swift[3] reported that the inelastic behavior of the adhesive layer must be considered in the residual strength analysis. It should be pointed out that the majority of the stress levels encountered in a typical design fatigue stress spectrum are significantly lower than the static design ultimate stress. Therefore, an elastic analysis will yield results of sufficient accuracy for fatigue crack growth life

analysis. This statement will be supported by the numerical demonstration described later in Sec. IV.

The 2-D shear spring element has been incorporated into an in-house stand-alone finite element computer program whose element library consists of a quadratic quadrilateral element and a linear-strain triangular element. In addition, a 2-D shear spring element corresponding to the linear-strain triangular element was developed utilizing the principles described previously in this section. The linear-strain element serves primarily as a filler element in constructing finite element meshes; most of the elements in the models are quadratic quadrilateral isoparametric elements.

III. Debonding

Experimental observation[1] indicated that debonding (cohesive failure) often occurs at a crack. The debonding will result in the loss of effectiveness of load transfer from the cracked adherend to the uncracked adherend. Thus, neglecting debonding will result in an underestimation of the stress intensity factor which, in turn, will lead to unconservative structural life prediction.

Following Ratwani,[1] the critical strain criterion is adopted to predict debonding. The effective shear strain $\bar{\epsilon}$ of an adhesive is defined as,

$$\bar{\epsilon}=\tfrac{2}{3}\sqrt{\gamma_{zx}^2+\gamma_{zy}^2} \tag{13}$$

When $\bar{\epsilon}=\epsilon_{cr}$, debonding occurs. ϵ_{cr} is the fracture strain obtained from simple tension test of adhesive. The nine Gaussian integration points within an element, Fig. 4, provide a convenient basis for predicting debonding. The $\bar{\epsilon}$ at each Gaussian integration point is evaluated and compared with ϵ_{cr} to determine debonding.

Two calculations are required to compute the stress intensity factor when considering debonding. In the first calculation, $\bar{\epsilon}$ is calculated to determine debonding. In the second calculation, debonding is incorporated into the calculation of element stiffness; if debonding occurs at a Gaussian integration point, the contribution of the particular point to the element stiffness is zero.

IV. Numerical Demonstration

The 2-D shear spring element was used in conjunction with the ¼ position collapsed quadratic quadrilateral isoparametric element developed by Barsoum.[4] This is an efficient approach to calculating the stress intensity factors, using a rather coarse mesh size, of the four types of specimens shown in Figs. 5-8. These four types of problems were chosen for numerical demonstration because there exist experimental data available from Ref. 1 for comparison. The dimensions of the four types of specimens and details about the experiment are described in Ref. 1.

In all of the finite element models established for Figs. 5-8, the mesh pattern and size on the cracked and uncracked adherends are exactly the same. However, there is no 2-D shear spring element between the ¼ position collapsed quadratic quadrilateral elements surrounding the crack tip and the corresponding linear strain triangular elements in the uncracked adherend. Figure 9 shows an example of a finite element model for the specimen shown in Fig. 5. For all the models, the ratio L/a, shown in Fig. 9, is about 0.04 ~ 0.05; and the ratio b/a is about 0.1, which Ref. 1 suggests as the aspect ratio of debonding.

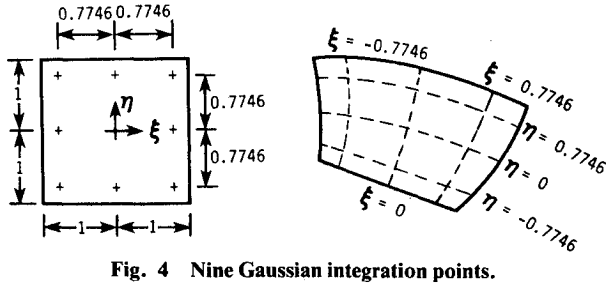

Fig. 4 Nine Gaussian integration points.

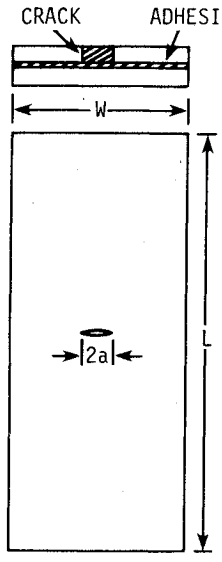

Fig. 5 Central crack specimen.

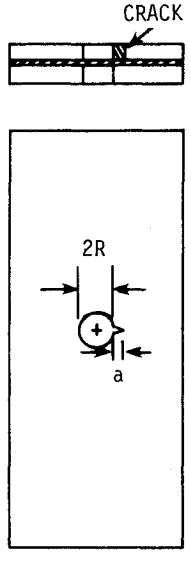

Fig. 6 Cracked hole specimen.

An important factor to be considered is the local transverse bending induced by the eccentricity of load transfer from cracked to uncracked adherends. Such local transverse bending is not included in the two-dimensional finite element analysis and, therefore, must be treated separately. Without the consideration of local transverse bending, an underestimation of the stress intensity factor will result and, in turn, will give unconservative structural life predictions. In accordance with Ref. 5, the effect of local transverse bending was incorporated into a bending correction factor, B_c. The B_c for the problems shown in Figs. 5-8 are given below.

Central crack (Fig. 5)

$$B_c=0.5\,a\,M \tag{14}$$

Cracked hole (Fig. 6)

$$B_c=0.125\,a\,G\,M \tag{15a}$$

$$G=\frac{1}{2}\left(1+\frac{1}{g}\right)\left[2-\left(\frac{1}{1+g}\right)^2-\left(\frac{1}{1+g}\right)^4\right] \tag{15b}$$

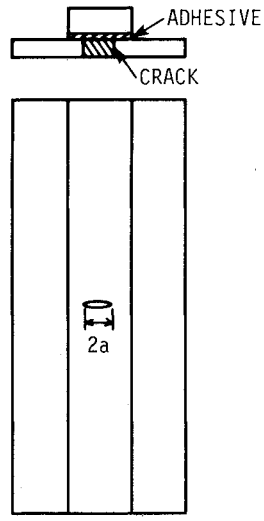

Fig. 7 Central stiffener specimen.

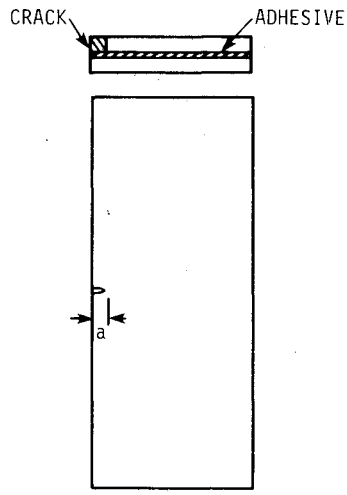

Fig. 8 Edge crack specimen.

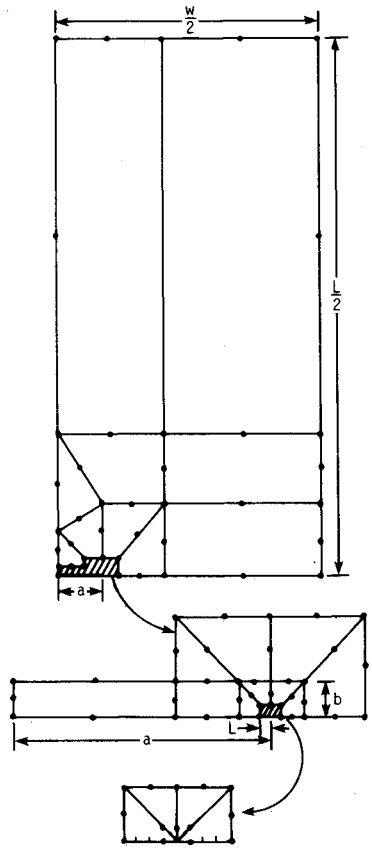

Fig. 9 Finite element model for ¼ of central crack specimen.

$$g = a/R \qquad (R = \text{radius}) \tag{15c}$$

Stiffened panel (Fig. 7)

$$B_c = 0.2905\, a\, M \tag{16}$$

Edge crack (Fig. 8)

$$B_c = 0.25\, a\, M \tag{17}$$

$$M = 1 - K_A/K_S = \text{load transfer factor} \tag{18}$$

where K_A and K_S are the stress intensity factors with and without load transfer, respectively. K_A is obtained from the finite element method described in Sec. II and III. K_S is calculated from the cracked adherend alone, without considering the adhesive layer and uncracked adherend.

The material property data used in the finite element analyses are exactly the same as those used in the experimental tests of Ref. 1. The material property data are shown below. The stress level used in the finite element analysis is also the same as that used in the experimental tests, i.e., 106.8 MPa (15.5 ksi).

Young's modulus of adherend	= 70.97 GPa (10.3×10^3 ksi)
Poisson's ratio of adherend	= 0.33
Shear modulus of adhesive	= 413.4 MPa (60.0 ksi)
Fracture strain of adhesive	= 0.04

The finite element results for the problems shown in Figs. 5-8 are shown in the corresponding Figs. 10-13. The experimental $K/(\sigma\sqrt{\pi a})$ is shown as an open symbol and the analytical $K/(\sigma\sqrt{\pi a})$ calculated with the 2-D shear spring element is shown as a solid symbol. It can be seen from Figs. 10-13 that the analytical and experimental results agree well. It should be mentioned that none of the models has more than 290 nodal points, yet they give quite accurate results. For example, the model shown in Fig. 9 for a center crack specimen has only 170 nodal points. The comparison shown in Fig. 10 indicates that the accuracy of computed stress intensity factor is very good. The same accuracy for a center crack specimen was also achieved in Ref. 5, nevertheless, using a model which has 233 nodal points. The effectiveness

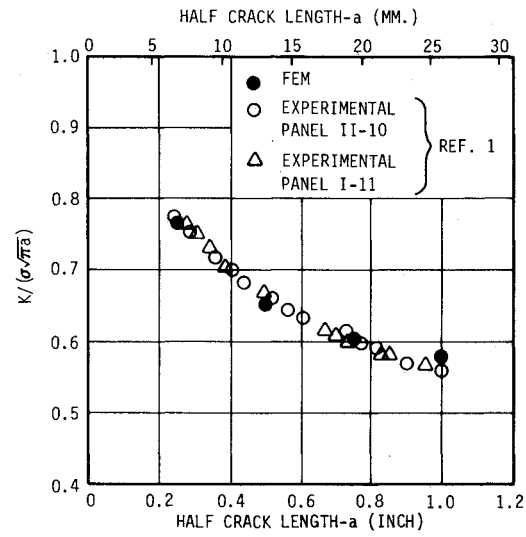

Fig. 10 Normalized K in central crack specimen.

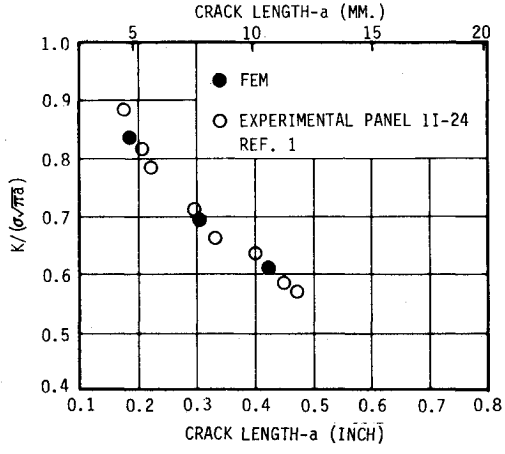

Fig. 11 Normalized K in cracked hole specimen.

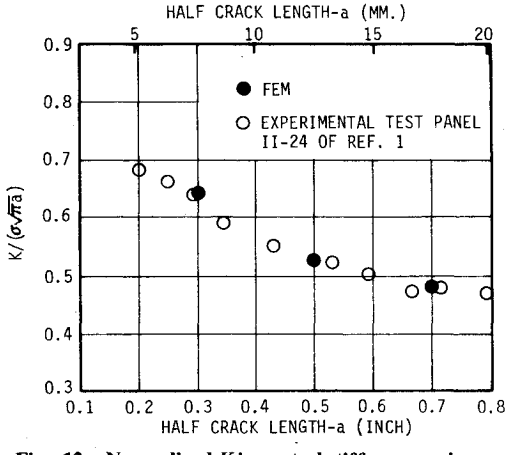

Fig. 12 Normalized K in central stiffener specimen.

of the 2-D shear spring element can be attributed to the fact that the element continuously transfers the load from cracked adherend to the uncracked adherend. Also, the preprocessing effort to calculate shear spring constant is not required; thus, it expedites analysis.

The problem in computing stress intensity factors of adhesively bonded structures is three-dimensional in nature. At present, using three-dimensional finite analyses to generate sufficient stress intensity factors for such a complex problem is practically prohibitive. The simple two-dimensional analysis reported herein appears to give quite an accurate stress intensity factor solution. Although the applicability of

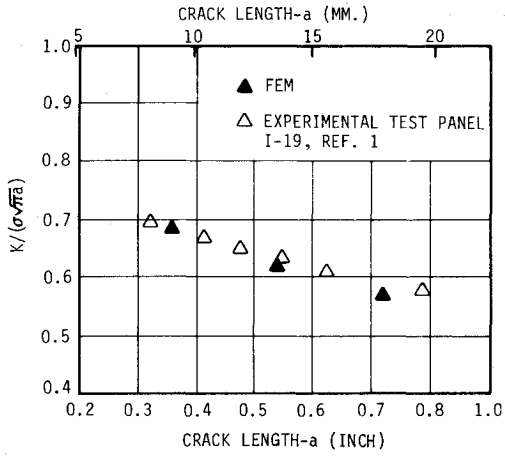

Fig. 13 Normalized K in edge crack specimen.

the new 2-D shear spring element to a model load-transfer medium was demonstrated only with the adhesively bonded structures, the new element is also expected to be applicable to modeling the honeycomb core of sandwich structures.

V. Conclusion

Based upon the comparison of analytical and experimental results, it is concluded that the new 2-D shear spring element has been demonstrated to be an accurate and convenient tool for modeling adhesive layers to compute the stress instensity factors.

Acknowledgment

The work reported herein was supported by the Fairchild Republic Company's CY 1982 Independent Research and Development Program.

References

[1] Ratwani, M. M., "Characterization of Fatigue Crack Growth in Bonded Structures," Vol. I, AFFDL-TR-77-31, June 1977.

[2] Zienkiewicz, O. C., *The Finite Element Method in Engineering Science*, 2nd Ed., McGraw-Hill Book Co., New York, 1971.

[3] Swift, T., "Fracture Analysis of Adhesively Bonded Cracked Panels," *Journal of Engineering Materials and Technology*, Vol. 100, Jan. 1978, pp. 10-15.

[4] Barsoum, R. S., "On the Use of Isoparametric Finite Elements in Linear Fracture Mechanics," *International Journal for Numerical Methods in Engineering*, Vol. 10, 1976, pp. 25-37.

[5] Ratwani, M. M., "Characterization of Fatigue Crack Growth in Bonded Structures," Vol. II, AFFDL-TR-77-31, June 1977.